Int. J. Nonlinear Anal. Appl.
Volume 11, Special Issue, Winter and Spring 2020, 211-230
ISSN: 2008-6822 (electronic)
http://dx.doi.org/10.22075/ijnaa.2020.4596

Optimal placement of charging station and distributed generation considering electricity price and load uncertainty using NSBSA algorithm

Seyed Masoud Alizadeh Masoumian[a*], Alireza Alfi[a], Ahmad Rezaee Jordehi[a]

[a] *Faculty of Electrical and Robotic Engineering, Shahrood University of Technology, Shahrood, 36199-95161, Iran.*

Abstract

In all developed countries, energy systems are being adapted to employ sustainable energies as such these countries are developing some programs to reduce the usage of fossil energy as much as possible in order to avoid environmental pollution and make the world a better place to live. The use of electrical vehicle (EV) is one of the appropriate options in this regard. In this paper, the power of charging stations, load uncertainty, and the uncertainty of electricity price in power systems were modeled using the behaviors of EV owners and a two-point estimate method, respectively. Then the contribution coefficient of charging stations and wind generation units as a distribution system were optimized using the NSBSA algorithm. Simulation was performed in MATLAB software, and IEEE 9-bus test system validated the efficiency of this algorithm.

Keywords: Charging Station, Wind Generator, NSBSA Algorithm.

1. Introduction

In today's societies, a direct relationship exists between the accessibility to new energy resources and the level of development in a country. Regarding limited energy resources in this era, the existing energy resources are not reliable anymore. Unrenewable fuels are the primary energy resources in a majority of countries worldwide, accounting for 80% of consumption and an 87% increase by 2030, according to the International Energy Agency's (IEA) statistic in 2016 [1]. There are concerns about the economic and political consequences of fossil resources and the excessive consumption of fossil resources, which are diminishing every day, and the fact that a large portion of environmental

*Corresponding Author: Seyed Masoud Alizadeh Masoumian
Email address: sma.masoumian@gmail.com (Seyed Masoud Alizadeh Masoumian[a*], Alireza Alfi[a], Ahmad Rezaee Jordehi[a])

Received: February 2020 *Revised:* August 2020

pollutions are caused by greenhouse gases such as CO2 and NOx. That is why men should spare their efforts to stop their dependency on fossil resources. For example, in a study by a Japanese company in Tehran, it was revealed vehicles account for 88% of air pollution [2]. This made researchers look for an appropriate solution to solve these kinds of troubles [3]. Using EVs and renewable resources can improve this situation significantly, regardless of their numerous difficulties. Now, energy-saving resources [4, 5] such as EVs' batteries are needed to be used at peak times to address this problem [6].

In [7], the EV owners' behaviors were examined, and it was found out that more than 90% of EVs are parked overnight. With considering Charging Stations (CSs) to connect this type of vehicles to grid, it is possible to provide additional power of grid, i.e. Vehicle to Grid (V2G), by discharging the vehicle's batteries at load peak hours, and the vehicle can be charged for personal applications at low load hours [8]. Controlling the charge and discharge procedure of vehicles is done by a smart grid. A smart grid represents the utilization of information technology and advanced communications to manage the energy consumption by consumers wisely. In other words, integrating information from various energy resources such as renewable energy resources, consumers, NOx, EVs must be identical to guarantee the network security and system stability, generation, and consumption [9]. On the other side, integrating EVs and Distributed Generation (DG) in power systems leads to peak dissipation, reduced network losses, reduced dependencies on upstream networks, and benefits to the EV owners.

Fulfilled programming of benefits from distribution system managers makes EVs be integrated with DG to save energy at specific times and deliver the energy at other times. With intellectual management of the charge and discharge of EVs' batteries and V2G-based system, the use of wind and sun energy in a power network would be more efficient [10]. In [11], it was argued that utilizing EVs' batteries to save the wind energy and deliver it to the network would affect the effective use of this renewable energy resource. There are similar findings about the effect of EVs on the usage of renewable resources in [12]. In [13], the interaction between the transportation system and power system with EVs was studied using the data available in the transportation system. In this study, it was revealed that V2G technology increases the flexibility of the power system and causes further usage of wind in power generation. The findings in [14] indicated that although EVs as energy savers may need further investments, they support renewable energy resources in power generation. In [15], the programming and operation of the power system in the presence of EVs were examined. In this study, it was revealed that the presence of V2G led to a 3% decrease in the programming and operation of the power system's costs in Northern Europe. Smart control strategies were adopted in the operation of EVs in [16]; however, load uncertainty and electricity prices have not been considered. In [17], the peak load was included as the main load of the network, and an hourly load model was proposed. In [18, 19, 20, 21], multiple placements of EVs' charging stations to minimize the objective function were studied; however, load modeling, strong objective function, and load uncertainty and electricity price were disregarded.

This paper is to analyze EVs as a distribution system (DS) and distributed generation units such as private organizations with regard to load uncertainty and electricity price and present a model using a two-point estimate method (2PEM) [22, 23] and power generation support with smart control to maximize the benefit function of both distribution system and private organization with contribution coefficient determined by optimization algorithm.

2. PROBLEM FORMULATION

In this paper, two objective functions are included, which encompass other sub-functions. To model these target functions, the parameters of electricity price, wind power, charging station system, and the behavior of electric vehicle owners need to be considered. In the first part of the simulation, the price curve, load, and wind are modeled based on the input and output values. In the second part, optimization is performed using the NSBSA algorithm. In this case, the two-point estimate method is used to obtain the electric and load price curves [24].

2.1. Uncertainty model

Regarding the wide application of DGs in the distribution network, various optimization methods are presented to find the optimal place and capacity of DGs. The load model and electricity price can significantly affect the pace and magnitude of the DGs' placement problem. Although load curve and electricity price are obtainable using the estimate methods, their curve variation as a percentage of error is not certainly specified. In this paper, the uncertainty of the load continuity curve and electricity price are modeled using normal distribution function probabilistically.

2.1.1. Load uncertainty

According to the probabilistic behavior of distribution network users in terms of electricity consumption, daily load variation is the amount of load consumed during the first year of the programming period. Each year of the programming period is divided into NDLF demand level (DL), and the duration of each DL is t,h level. The second parameter of the load model is demand level factor (DLF), which can be obtained using probability density function (PDF) as follows [25]:

$$DLF^{e}_{i,t,h} = \mu^{D}_{i,t,h} + \lambda^{D,e}_{i,t,h} \times \sigma^{D}_{i,t,h} \tag{2.1}$$

where, λ is a stochastic variable with standard deviation of and mean value of zero and a normal distribution function for each DL. μ and σ are the estimated values of load demand level and their standard deviation, respectively. The load demand curve can be obtained using Equation (2.6). Considering the load growth rate γ for each year t during the program period, electricity consumption level in at each DL can be calculated as follows [25]:

$$P^{D,e}_{i,t,h} = P^{D}_{i,base} \times DLF^{e}_{h} \times (1+\gamma)^{t} \tag{2.2}$$

$$Q^{D,e}_{i,t,h} = Q^{D}_{i,base} \times DLF^{e}_{h} \times (1+\gamma)^{t} \tag{2.3}$$

$$S^{D,e}_{i,t,h} = P^{D}_{i,t,h} + jQ^{D,e}_{i,t,h} \tag{2.4}$$

$$S^{D}_{i,base} = P^{D}_{i,base} + jQ^{D}_{i,base} \tag{2.5}$$

$$\sigma^{D}_{i,t,h} = 0.01 \times \mu^{D}_{i,t,h} \tag{2.6}$$

2.1.2. Electricity price uncertainty

According to electricity consumption level and the behavior of electricity market operator, the purchased electricity of the main network is priced for customers. The electricity price changes during each period of the program. The variations of this quantity can be modeled by multiplying two parameters, i.e., the base price of electricity for each DL and price level factor [26, 27, 28]:

$$\rho_{t,h} = \rho \times PLF^{e}_{t,h} \tag{2.7}$$

Price level factor (PLF) represents the behavior of the electricity market, and probability density function can be calculated as follows [29]:

$$PLF^{e}_{t,h} = \mu^{\rho}_{t,h} + \lambda^{\rho,e}_{i,t,h} \times \sigma^{\rho}_{t,h} \tag{2.8}$$

where, λ is a stochastic variable produced by standard deviation of one and mean value of zero for each DL, μ and σ are the estimated values of PLF and their standard deviation, respectively. Price level curve is obtained by Equation (2.9). Figure 1 shows the PLF coefficient for 24 hours, and the DLF coefficient for nine buses (case study) for 24 hours [30].

$$\sigma^{\rho}_{t,h} = 0.1 \times \mu^{\rho}_{t,h} \tag{2.9}$$

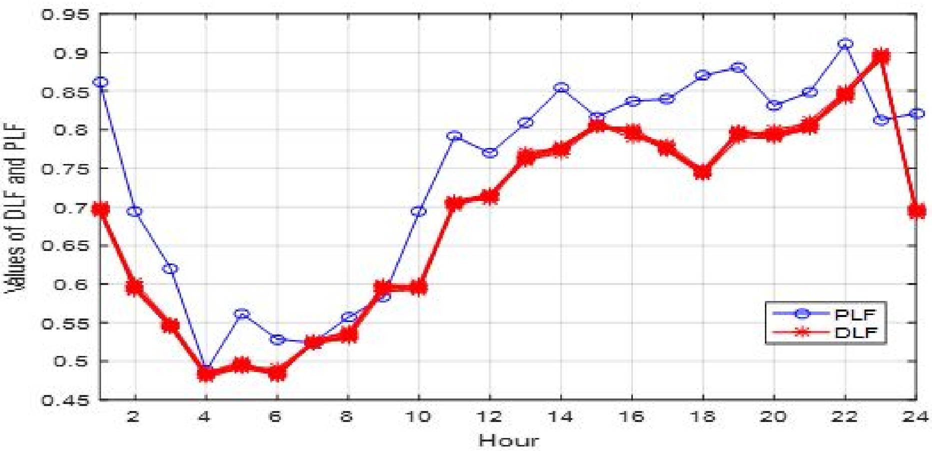

Figure 1: DLF and PLF for daily period

2.2. Wind generator unit

Power generation depends on wind velocity factor in the concerned region. This parameter has no certain value and is selected stochastically. Accordingly, the DG placement also depends on how the parameter is modeled. In this case, several experiments were performed to show how Rayleigh probability density function is the best option for modeling the stochastic behavior of wind velocity. Rayleigh density function is a specific state of Weibull distribution function, which has the shape index of 2 [31].

$$F(x,y,z) = \frac{y}{z} \times (\frac{x}{z})^{y-1} \times e^{-(\frac{x}{z})^{y}} \xrightarrow[x=v,c=z]{y=2} f_{wg}(v) = (\frac{2v}{c^2}) \times e^{\left(-(\frac{v}{c})^2\right)} \tag{2.10}$$

where, v and c are wind velocity and scaling index of Weibull distribution, respectively. The average value of wind velocity during 24 hours is shown in Figure 2.

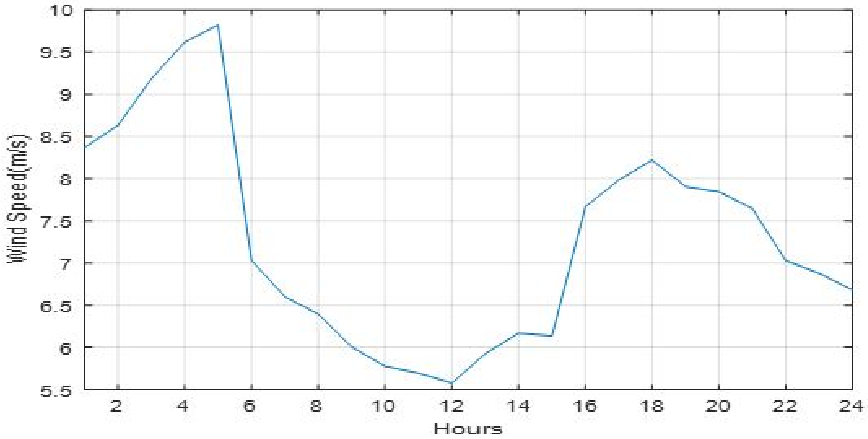

Figure 2: Average value wind speed for daily

If the average value of wind velocity is obtained, the scaling index is then calculated, and the mentioned distribution function corresponds to Figure 3.

$$v_m = \int_0^\infty v \cdot f_{wg}(v)dv = \int_0^\infty \left(\frac{2v^2}{c^2}\right) e^{\left(-\left(\frac{v}{c}\right)^2\right)} dv = \frac{\sqrt{\Pi}}{2} c \longrightarrow c \cong 1.12837 v_m \tag{2.11}$$

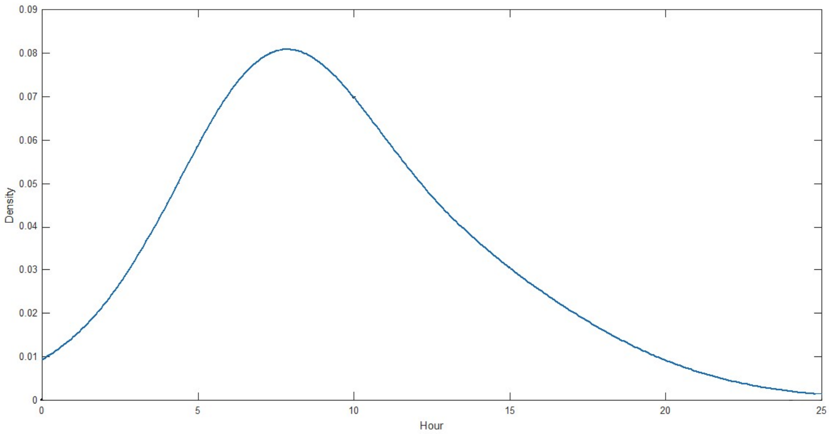

Figure 3: wind speed Weibull distribution function

After modeling the wind velocity, the power generated by wind turbines can be obtained by Equation (2.12) [32].

$$P_{i,t,h}^{wg} = \begin{cases} 0 & \text{if} \quad v \le v_{in}^{cut} \ or \ v \ge v_{out}^{cut} \\ P_{i,r}^{wg} \frac{v - v_{in}^{cut}}{v_{rated} - v_{in}^{cut}} & \text{if} \quad v_{in}^{cut} \le v \le v_{rated} \\ P_{i,r}^{w} & \quad else \end{cases} \tag{2.12}$$

where, $P_{i,t,h}^{wg}$ is the authorized capacity of power generation in wind unit. v_{in}^{cut}, v_{out}^{cut} and v_{rated}^{cut} are cut in, cut out, and rated speed of wind turbine for power generation, respectively.

2.3. Modeling charging station power

Charging station power depends on scheduling the charging manner of vehicle and other factors such as capacity and kind of vehicles' batteries, the initial charge of vehicles' batteries, and vehicles present in the charging station. These parameters have no certain values and are stochastic. The EV owners' behaviors mostly affect the modeling of these uncertain parameters, in comparison to the other factors. Capacity and kind of EVs' batteries, which are different from the ones having been produced by vehicle companies up to now. The capacity for vehicles' batteries was considered to be 30 KW in this study. The lifetime of batteries was estimated to be about 5 years [33]. Accessibility of each vehicle at each hour depends on the time when the vehicle enters and exits from the charging station. These two times are both stochastic and caused by human behavior. Vehicles' entrance time to a charging station and their exit from parking lot must be obtained using vehicle reference to charging stations with V2G capability data. For this purpose, to consider the effect of the stochastic nature of time when vehicles obtain the output power of the charging station and to avoid incorrect estimations, it is more practical to fit the data presented in Figure 4 in the form of normal distribution. As presented in Figure 5, the mean, standard deviation, and variance of the normal distribution yield are 4.3854, 3.6897, and 13.6140, respectively. In this paper, the arrival time of each vehicle to the charging station was obtained from the normal distribution function.

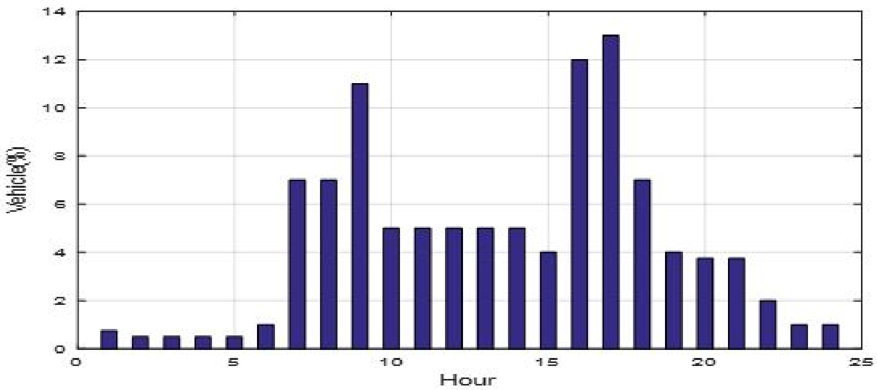

Figure 4: Presence of vehicles in charging station by hour [32]

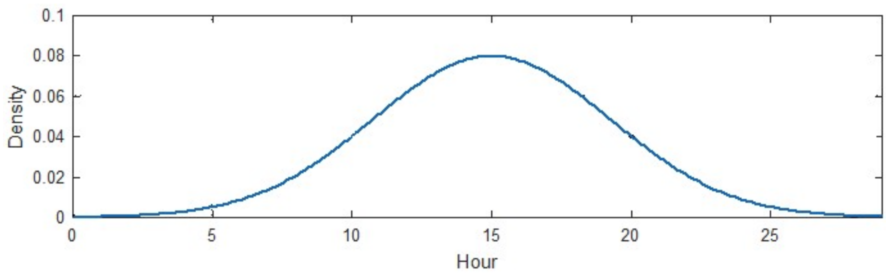

Figure 5: PDF for state of charge

The initial value of vehicle battery, i.e. the ratio of energy stored in the battery to its capacity, has a value ranging from 0 to 100. When the vehicle battery is charged, the equivalent value increases; however, the consumption of the battery energy (delivering power to grid or driving) decreases the initial charge value. The storage capability of batteries is not used when the vehicle is in the charging station. According to the stochastic nature of distance traveled by vehicles, efficiency, and kind of vehicles' battery, the initial value of remained energy in the vehicle's battery is stochastic as well. In this study, the initial charge value of the vehicles referring to the charging station was considered at three levels, as shown in Figure 6.

Scheduling the vehicle's charging process is determined upon the request of the vehicle owner at its entrance of each vehicle to the charging station, initial charge level, final charge level asked, and exit time of each vehicle from the charging station. Then, considering this information and the benefit resulted from deploying vehicles as storage devices, the benefits from charging the batteries for driving, optimal charge and discharge schedule for a vehicle at the present time at a charging station are determined. Time required for complete charge and discharge of vehicles' battery can be calculated using initial charge value by Equations (2.13)-(2.14) [34].

$$t_{charge}(j) = \frac{(SOC_{\max} - SOC_j) \times ES_j}{P_v} \tag{2.13}$$

$$t_{discharge}(j) = \frac{(SOC_j - SOC_{\min}) \times ES_j}{P_v} \tag{2.14}$$

where, SOC stands for State of Charge, and $SOC_{\max}$, and SOC_{min} are maximum and minimum charging values of the vehicle's battery. ES is the vehicle's battery capacity. P_v is the power received by EV to be charged. This section presents mathematical modeling of charging station power [35].

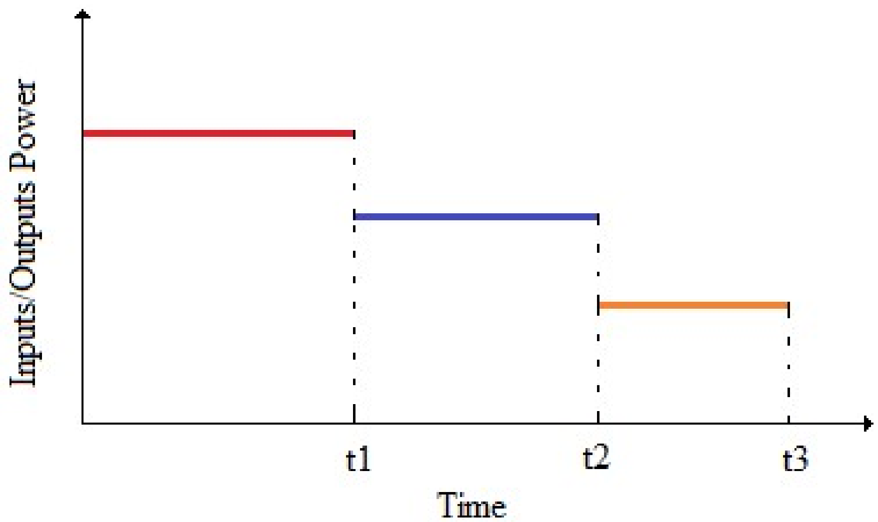

Figure 6: Modeling input and output power of charging station (three levels)

$$\begin{aligned} P_{charge} = \sum_{i=1} N_i \times P_{vi} \times ES \times \Big[&\big(n_{charge1} + n_{charge2} + n_{charge3}\big) \times \big(SOC_{\max} - SOC_{charge3}\big) + \\ &\big(n_{charge1} + n_{charge2}\big) \times \big(SOC_{charge3} - SOC_{charge2}\big) + n_{charge3} \times \big(SOC_{charge2} - SOC_{charge1}\big)\Big] \end{aligned} \tag{2.15}$$

$$\begin{aligned} P_{discharge} = \sum_{i=1} N_i \times P_{vi} \times ES \times \Big[&\big(n_{discharge1} + n_{discharge2} + n_{discharge3}\big) \times \big(SOC_{discharge1} - SOC_{\min}\big) \\ &+ \big(n_{discharge1} + n_{discharge2}\big) \times \big(SOC_{discharge2} - SOC_{discharge1}\big) \\ &+ n_{discharge3} \times \big(SOC_{discharge3} - SOC_{discharge2}\big)\Big] \end{aligned} \tag{2.16}$$

N and P_{vi} are capacity and vehicle presence percentage, respectively. $n_{dischargei}$ and $n_{chargei}$ are the number of vehicles with an initial charge of $SOC_{\max}$ and $SOC_{\min}$ at i^{th} charging station.

2.4. Objective function

The objective function consisting of OF1 and OF2. OF1 is distribution system manager (DS) benefit and OF2 is wind generator (WG) benefit. The coefficient K is used to participate in the two functions. DS received a 0.05×10^7 \$ contribution from WG as a cooperation.

$$OF1 = (1 - K) \times B_{wg} + B_{cs} + 500000 \tag{2.17}$$

$$OF2 = WG + K \times B_{wg} - 500000 \tag{2.18}$$

2.4.1. Charging station's investment cost

Charging station's installation costs encompass charging station's equipment cost, wages, charging station's construction cost, and charging station's place cost. These costs are calculated in accordance with Equation (2.19) and the benefit function of the distribution system manager (2.20). Furthermore, the inflation rate and benefit rate have been considered in these functions [34].

$$C_{total}^{inv} = \sum_{i=1}^{N_{cs}} \left(C_i^{equip} + C_i^{construction}\right) \times CP_i = \sum_{i=1}^{N_{cs}} C_{ac} \times CP_i \tag{2.19}$$

$$DS = B_{total}^{charge} + B_{total}^{discharge} + B_{total}^{load} + B_{total}^{loss} + B_{total}^{reliability} - C_{total}^{inv} \tag{2.20}$$

2.4.2. Benefits of charging

Regarding the EV drivers, charging station managers can increase the benefits by presenting charging services. To this end, the benefit resulted from recharging the vehicle's battery can be obtained from Equation (2.23) [36].

$$R_{total}^{charge} = \sum_{t=1}^{T} \sum_{h=1}^{N_h} \sum_{i=1}^{N_{cs}} \rho_{t,h} \times P_{i,t,h}^{cs} \times \tau_{t,h} \times \left(\frac{1 + InfR}{1 + IntR}\right)^t \tag{2.21}$$

$$C_{total}^{charge} = \sum_{t=1}^{T} \sum_{h=1}^{N_h} \sum_{i=1}^{N_{cs}} \left(\frac{\rho_{t,h,pur}^{grid}}{\mu_{conv}} + c_d\right) \times P_{i,t,h}^{cs} \times \tau_{t,h} \times \left(\frac{1 + InfR}{1 + IntR}\right)^t \tag{2.22}$$

$$B_{total}^{charge} = R_{total}^{charge} - C_{total}^{charge} \tag{2.23}$$

2.4.3. Benefits of discharging

At peak times, the battery can provide less expensive energy to contribute to the network, compared with the upstream network's energy [37]. The benefits from V2G technology can be obtained from Equation (2.26).

$$R_{total}^{discharge} = \sum_{t=1}^{T} \sum_{h=1}^{N_b} \sum_{i=1}^{N_{cs}} \rho_{t,h} \times P_{i,t,h}^{cs} \times \tau_{t,h} \times \left(\frac{1 + InfR}{1 + IntR}\right)^t \tag{2.24}$$

$$C_{total}^{discharge} = \sum_{t=1}^{T} \sum_{h=1}^{N_b} \sum_{i=1}^{N_{cs}} \left(\frac{\rho_{t,h,pur}^{EV}}{\mu_{conv}} + C_d\right) \times P_{i,t,h}^{cs} \times \tau_{t,h} \times \left(\frac{1 + InfR}{1 + IntR}\right)^t \tag{2.25}$$

$$B_{total}^{discharge} = R_{total}^{discharge} - C_{total}^{discharge} \tag{2.26}$$

C_d is equipment depreciation cost posed by V2G and efficiency rate of charging station inverters.

2.4.4. Benefits from power provided by an upstream network

Most of the distribution network is fed by an upstream network. With the inclusion of charging stations, the power level is reduced. It would then reduce the purchased power costs and consequently increase the benefits of distribution system manager.

$$R_{total}^{load} = \sum_{t=1}^{T} \sum_{h=1}^{N_h} \rho_{t,h} \times P_{t,h}^{load} \times \tau_{t,h}^{load} \times \left(\frac{1 + InfR}{1 + IntR} \right)^t \tag{2.27}$$

$$C_{total}^{load} = \sum_{t=1}^{T} \sum_{h=1}^{N_h} \rho_{t,h}^{grid} \times P_{t,h,pur}^{grid} \times \tau_{t,h}^{grid} \times \left(\frac{1 + InfR}{1 + IntR} \right)^t \tag{2.28}$$

$$B_{total}^{load} = R_{total}^{load} - C_{total}^{load} \tag{2.29}$$

$$P_{t,h}^{grid} = \begin{cases} P_{t,h}^{load} + P_{t,h}^{loss} - \sum_{i=1}^{N_{cs}} P_{i,t,h}^{cs} & \text{for peak demand levels} \\ P_{t,h}^{load} + P_{t,h}^{loss} + \sum_{i=1}^{N_{cs}} P_{i,t,h}^{cs} & \text{for medium demand levels} \\ P_{t,h}^{load} + P_{t,h}^{loss} + \sum_{i=1}^{N_{cs}} P_{i,t,h}^{cs} & \text{for low demand levels} \end{cases} \tag{2.30}$$

2.4.5. Benefits from reducing active power losses

With the inclusion of DG units and V2G to the distribution network, the losses will be reduced. The benefits resulted from electricity sold to customers would be enhanced for the distribution system manager. This can be calculated from Equation (2.31) [34].

$$B_{total}^{loss} = \sum_{t=1}^{T} \sum_{h=1}^{N_h} \left[\left(Ploss_{t,h}^{\text{without CS and WG}} - Ploss_{t,h}^{\text{with CS and WG}} \right) \times \rho_{t,h} \times \tau_{t,h} \right] \times \left(\frac{1 + InfR}{1 + IntR} \right)^t \tag{2.31}$$

2.4.6. Benefits from reliability improvement

During the programming period, the distribution network faces troubles such as electricity outage and variation in reliability factors, which consequently lead to lots of detriments. With improving these factors, the distribution system manager's benefits can be increased, as illustrated in Equation (2.33) [38]. In this study, energy not-supplied (ENS) factor was used.

$$C_{ENS} = \left[\sum_{l=1}^{N_l} C_{int} \times \lambda_l \times L_l \times \left(\sum_{res=1}^{N_{res}} P_{res} \times t_{res} + \sum_{rep=1}^{N_{rep}} P_{rep} \times t_{rep} \right) \right] + C_{equip} \tag{2.32}$$

$$B_{total}^{reliability} = \sum_{t=1}^{T} \left[\left(C_{ENS}^{\text{without CS and WG}} - C_{ENS}^{\text{with CS and WG}} \right) \right] \times \left(\frac{1 + InfR}{1 + IntR} \right)^t \tag{2.33}$$

2.4.7. Resulted benefits and investment cost from DG units' operation (wind unit)

Wind unit's operation cost includes fuel cost and annual maintenance costs. Fuel cost was ignored in this study. The benefit from the wind unit can be obtained from Equation (2.38) [39].

$$WGC = \sum_{t=1}^{T} \sum_{h=1}^{N_h} \sum_{i=1}^{N_b} \sum_{wg=1}^{N_{wg}} \left(P_{i,t,h}^{wg} \times OC_{wg} \times \tau_{t,h} + Cost_{main,wgi} \right) \times \left(\frac{1 + InfR}{1 + IntR} \right)^t \tag{2.34}$$

$$WGR = \sum_{t=1}^{T} \sum_{h=1}^{N_h} \sum_{i=1}^{N_b} \sum_{wg=1}^{N_{wg}} \left(P_{i,t,h}^{wg} \times \rho_{t,h} \times \tau_{t,h}\right) \times \left(\frac{1+InfR}{1+IntR}\right)^{t} \tag{2.35}$$

$$WGB = WGR - WGC \tag{2.36}$$

$$WGIC = \sum_{t=1}^{T} \sum_{h=1}^{N_h} \sum_{i=1}^{N_b} \sum_{wg=1}^{N_{wg}} \left(S_{i,\max}^{wg} \times IC_{wg}\right) \times \left(\frac{1+InfR}{1+IntR}\right)^{t} \tag{2.37}$$

$$WG = WGB - WGIC \tag{2.38}$$

2.5. Load flow method and problem constraints

Newton-Raphson method was selected for load flow. For each h-DL, load flow relationships were calculated for each year of the programming period. Furthermore, the constraints of the voltage and current running through the distribution network equipment were considered at each level [27].

$$P_{t,h}^{grid} \pm P_{i,t,h}^{cs} + P_{i,t,h}^{wg} - P_{i,t,h}^{D\cdot e} - V_{i,t,h}^{e} \sum Y_{ij} V_{j,t,h}^{e} \times \cos\left(\delta_{i,t,h}^{e} - \delta_{i,t,h}^{e} - \theta_{ij}\right) = 0 \tag{2.39}$$

$$Q_{t,h}^{grid} - Q_{i,t,h}^{D\cdot e} - V_{i,t,h}^{e} \sum Y_{ij} V_{j,t,h}^{e} \times \sin\left(\delta_{i,t,h}^{e} - \delta_{i,t,h}^{e} - \theta_{ij}\right) = 0 \tag{2.40}$$

$$I_{l,t,h} \leq I_{\max}^{l}, \quad S_{t,h}^{grid} \leq S_{\max}^{grid} \tag{2.41}$$

$$V_{\min} \leq V_{i,t,h}^{e} \leq V_{\max} \tag{2.42}$$

$$P_{i,t,h}^{wg} \leq P_{i\max}^{wg}, \quad i = 1, 2, 3, \cdots, N_b, \;\; CP \leq CP_{\max} \tag{2.43}$$

3. PROPOSED NSBSA ALGORITHM AS A SOLUTION METHOD

In this paper, non-dominated sorting backtracking algorithm (NSBSA) was used to solve the optimization problems. The expansion of this algorithm in accordance with previous studies made the search algorithm more efficient. This algorithm is population-based and encompasses five procedures [40].

Algorithm NSBSA
Initialization
repeat
  2.Selection 1
    Generation of Trial-Population
      3.Mutation
      4.Crossover
  end
5.Selection 2
    until stopping conditions are met

Unlike lots of search algorithms, NSBSA has an individual control parameter and its simple structure can solve multi-model problems fast. Also, NSBSA can adapt to various kinds of numerical optimization problems [35, 40].

```
Control Mechanism of NSBSA
Input: T, Search space limits (i.e.,lowj, upj)
Output: T
for i from 1 to N do
  for j from 1 to D do
   if (Ti,j < lowj) or (Ti,j > upj) then
    Ti,j=rnd.(upj-lowj)+lowj
   end
  end
end
```

In this optimization, NSBSA, which is an unconscious search strategy and uses two searches simultaneously, was used to maximize the benefit. One of the searches is executed from the starting state to the objective state, and the other one is executed from the objective state to the starting state [40]. Instead of analyzing the objective test, NSBSA analyzes whether the boundaries of searches cross each other or not. If yes, the solution is obtained.

The selection criterion in NSBSA is a recognized ad quality factor with a rank parameter. The solution set is ranked at the beginning to be selected, and the solution with a lower rank has a better quality. Ranking is done using the dominant mechanism. In other words, solution sets dominating the other solutions, not their members, will be arranged with the same rank in Pareto front [41, 42, 43].

$$x \ \text{dom} \ y \Longleftrightarrow \begin{array}{l} \forall\, i : x_i \geq y_i \\ \exists\, i_0 : x_{i_0} \succ y_{i_0} \end{array} \tag{3.1}$$

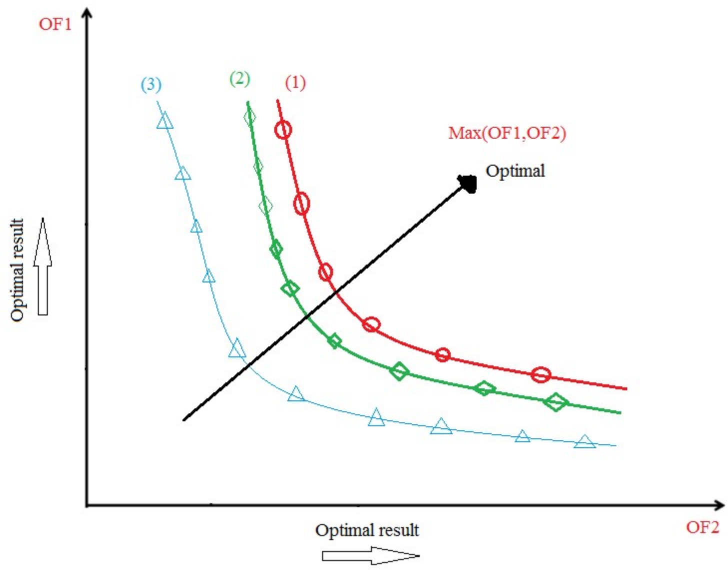

Figure 7: Solutions ranking [41, 42, 43]

Moreover, after collocating the solutions based on the ranking, selection will be based on crowding distance. This means that the selection criterion is the crowding distance of similar ranks. Crowding distance illustrates that more solutions result in more variation in Pareto front. The mathematical expression of this parameter is in accordance with Equations (3.1)-(3.2) and Figures 7-8.

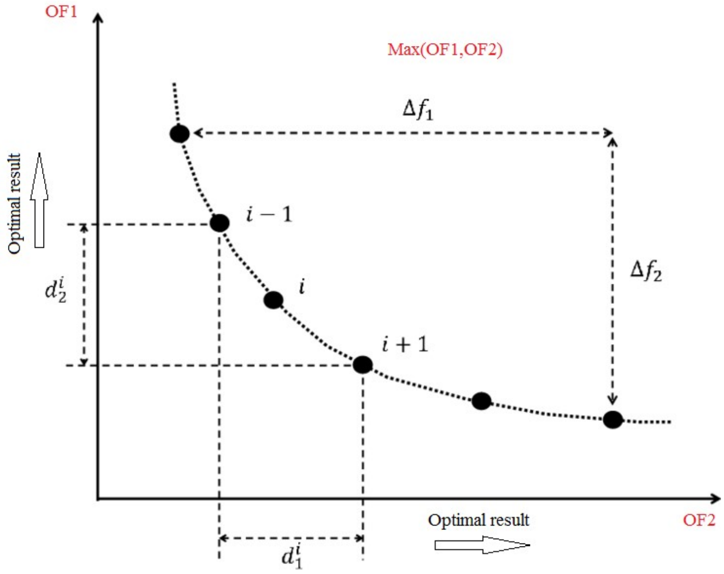

Figure 8: Crowding Distance [41, 42, 43]

$$d_i = \frac{\left|OF_1^{i+1} - OF_1^{i-1}\right|}{\left|OF_1^{\max} - OF_1^{\min}\right|} + \frac{\left|OF_2^{i+1} - OF_2^{i-1}\right|}{\left|OF_2^{\max} - OF_2^{\min}\right|} \tag{3.2}$$

3.1. Under study network and parameters required for simulation

In this study, IEEE 9-bus system was used. The model and the parameter of the concerned network are shown in Figure 9 and Table 1.

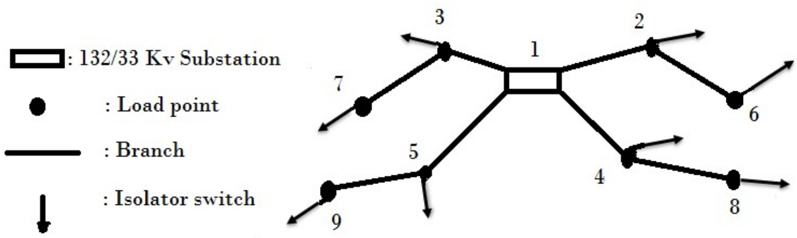

Figure 9: Nine-bus test system [34]

Table 1: Network information of case study [34]

Bus		Resistance (ohm)	Reactance (ohm)	Line length (Km)	Load (MW)
1	3	1.4	1.5	1.5	6
3	7	2.78	5.5	5.5	8.8
1	2	2	4	4	11.2
2	6	2.8	5.5	5.5	5
1	5	1.7	1.7	1.7	8.8
5	9	2.1	4	4	10.2
1	4	2.26	4.5	4.5	7
4	8	2.4	5	5	8.7

All the load points can be selected as candidate buses to install the DG units. The maximum and minimum values of the authorized capacity of wind generation units and charging stations were 1-6 MW and 100-600 vehicles, respectively. Placement was programmed for 10 years, and each phase of the programming period was divided into 24 DL. In the abovementioned DL, 365 days per year was assumed.

Table 2: Required information and values [32]

value	units	Parameter
4	%	Demand growth rate-γ
0.9	Per Unit	Minimum magnitude of voltage
1.1	Per Unit	Maximum magnitude of voltage
0.03	Fault/Km	Fault rate in line-λ_l
0.5	Hour	Timeout during error location-t_{rep}
3	Hour	Duration during fix error-t_{res}
5	%	Inflation rate - InfR
6	%	Interest rate - IntR
5	m/s	V_{in}^{cut}
35	m/s	V_{out}^{cut}
20	m/s	V_{rated}^{cut}

Table 3: CS Data [32]

value	units	Parameter
85-90-95	SOC1,2,3	Initial charging of vehicles
25-25-50	%	Number of charging Vehicle
10-12.5-15	SOC1,2,3	Initial discharging of vehicles
35-40-25	%	Number of discharging Vehicle
10	Kw	Charging/discharging power rate
95	%	Vehicle to Grid equipment-μ_{conv}

Table 4: Information electricity market [32]

value	units	Parameter
68	$/MWh	Electricity wholesale purchase price
0.18	$/MWh	Base price ENS
83	$/MWh	base price electricity retail sell-ρ
28	$/MWh	Operating cost of WGs - OC_{wg}
64	$/MWh	Electricity purchase price from vehicle
0.001	$/MWh	Degradation cost of V2G
72	$/MWh	Electricity price of sold to costumers
121	$/MWh	Price of energy not supply

4. SIMULATION RESULTS AND DISCUSSION

Simulation was performed in two scenarios. First, the contribution coefficient, K, was set to be zero, indicating that, with regard to the private organizations' investment, these organizations do not contribute to the distribution system manager, and that the resulting benefit from network's supplied power is gathered by the distribution system manager. The performance of these organizations is presented in Table 5.

Table 5: Optimal pareto front of scenario $I \times 10^7$ \$ with K=0

solution	OF1	OF2	C.D
1	4.5786	-0.4114	Inf
2	1.0008	-0.1122	Inf
3	3.7014	-0.1496	0.7132
4	2.6581	-0.1870	0.6522
5	4.5633	-0.3740	0.6045
6	4.2047	-0.2614	0.5966
7	3.3982	-0.2244	0.5609
8	3.7705	-0.2618	0.3504

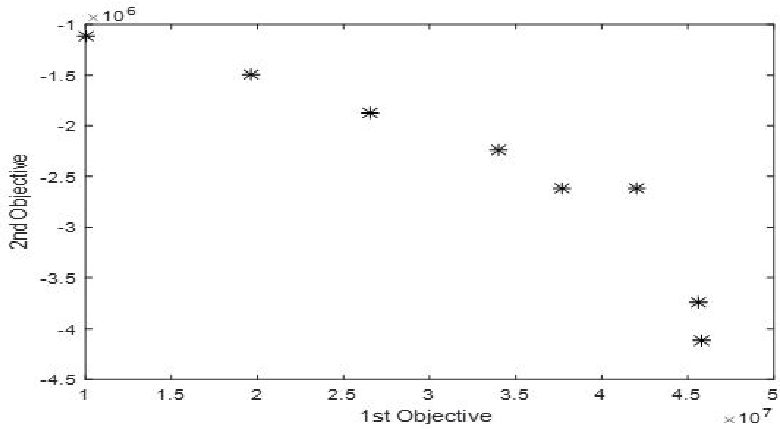

Figure 10: Optimal Pareto front (K=0)

Table 6: Optimal place/capacity of CS and WG units

Charging Station			Wind Generator		
Number	bus	Capacity(Vehicle)	Number	bus	Capacity(MW)
1	6	130	3	6	1
				8	1
				9	2

Table 7: Benefits for DS and WG $\times 10^7$ \$

Optimal	Bdis	Bch	Bup	Bloss	Br
3	0.0548	0.0107	1.1522	1.1024	0.0009

As it appears to be competently logical, the contribution of the private organizations is 0%. Although these organizations had invested, they played no role in the operation. Accordingly, their benefit function was negative. The best state in the third solution has a CD factor of 0.7132.

A more optimal solution is obtained by increasing this factor. Using the concerned optimization method, the benefit in the 3rd solution was 0.0090+06 \$ from reliability function, 11.5220e+06 \$ from upstream network function, 11.0240e+06 \$ from reduced active power losses, 0.1070e+06 \$ from charging function, 0.5480e+06 \$ from discharging function in the 10th year. In the second scenario, the contribution coefficient was generated stochastically by software. The installation place and capacity of private organizations and distribution system managers are presented in Tables 8 and 9, respectively.

Table 8: Optimal Pareto front of scenario $II \times 10^7$ \$ with K

solution	**OF$_1$**	**OF$_2$**	**K**	**C.D**
1	5.0693	-1.8786	0.1021	Inf
2	2.3926	2.6988	0.9986	Inf
3	3.3412	1.7572	0.6874	0.3128
4	3.0710	2.0484	0.7836	0.2989
5	4.6530	0.4510	0.2410	0.2746
6	4.2222	0.8707	0.3819	0.2465
7	4.0789	1.0125	0.4299	0.2237
8	3.4950	1.6027	0.6349	0.2231
9	2.6697	2.4420	0.9183	0.2187
10	3.9134	1.1835	0.4923	0.2154
11	3.5948	1.3867	0.5533	0.2071
12	5.0593	0.0524	0.1068	0.2063
13	2.5130	2.5675	0.9665	0.1925
14	3.7879	1.3206	0.5362	0.1894
15	2.8321	2.2802	0.8608	0.1892
16	4.4217	0.6705	0.3173	0.1769
17	4.8554	0.2502	0.1732	0.1706
18	2.9362	2.1832	0.8293	0.1696
19	4.4689	0.6260	0.3025	0.1625
20	4.8940	0.2186	0.1628	0.1447

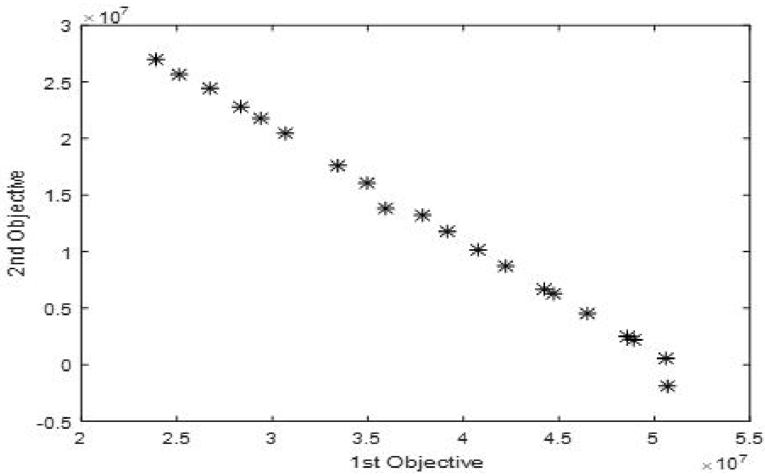

Figure 11: Optimal Pareto front of K

Table 9: Optimal place/capacity of CS and WG units

Charging Station			Wind Generator		
Number	**bus**	**Capacity(Vehicle)**	**Number**	**bus**	**Capacity(MW)**
1	2	312	3	6	1
				8	6
				9	1

Table 10: Benefits for DS and WG $\times 10^7$ \$

Optimal	Bdis	Bch	Bup	Bloss	Br
3	0.0421	0.0081	2.6576	2.9166	0.0206

The results indicate that the first and second solutions have infinite crowding distance as such they are not appropriate solutions, and the third solution with crowding distance of 0.3128 is an optimal solution. In this solution with a contribution factor of 68.74%, the benefits from distribution system (CS) and private organization (WG) are 33412000 \$ and 17572000 \$, respectively. Three DG units and a charging station were modeled in a network (Table 9). Moreover, the benefits from the optimization method are presented in Table 10. Using this optimization method in the 3rd solution, the benefits were 0.2060e+06 \$ from reliability function, 26.5760e+06 \$ from upstream network function, 29.1660e+06 \$ from reduced active power losses, 0.0810e+06 \$ from charging function, and 0.4210e+06 \$ from discharging function in the 10th year. Figure 12 shows the profits from the reliability function in the presence of CS and WG in the first, third, sixth, and tenth years for a 24-hour daily period, according to which better results are obtained in the 10th year, and the highest profit (6.5062e+05 \$) was made in the 10th year.

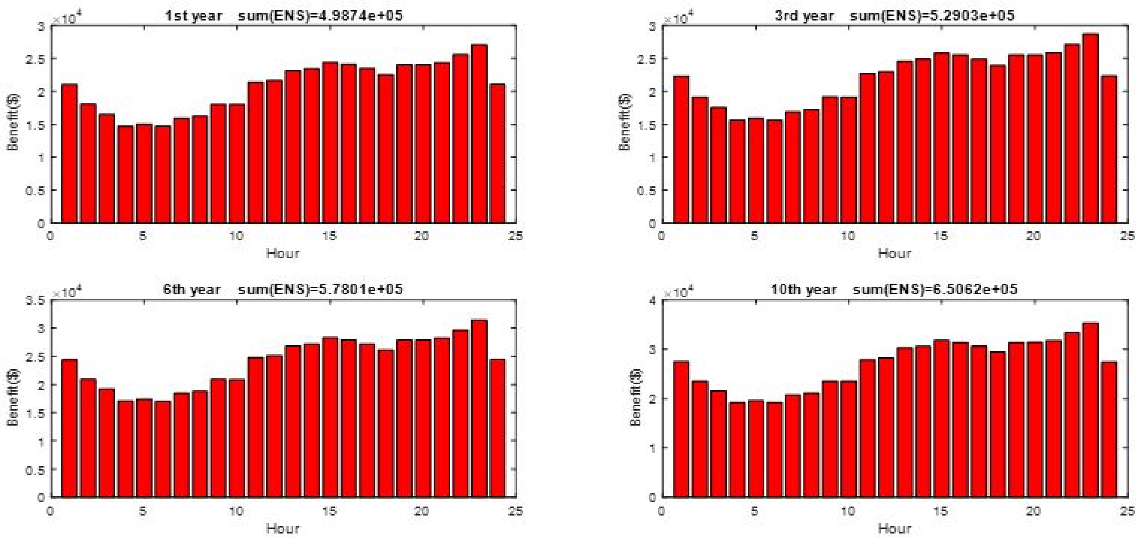

Figure 12: Benefits from reliability function in a short time (with CS and WG)

Figure 13 shows the profit resulting from a decrease in active power losses. Planning led to the highest profit in the 10th year (3.1777e+06 \$). CS and WGs are involved in such planning.

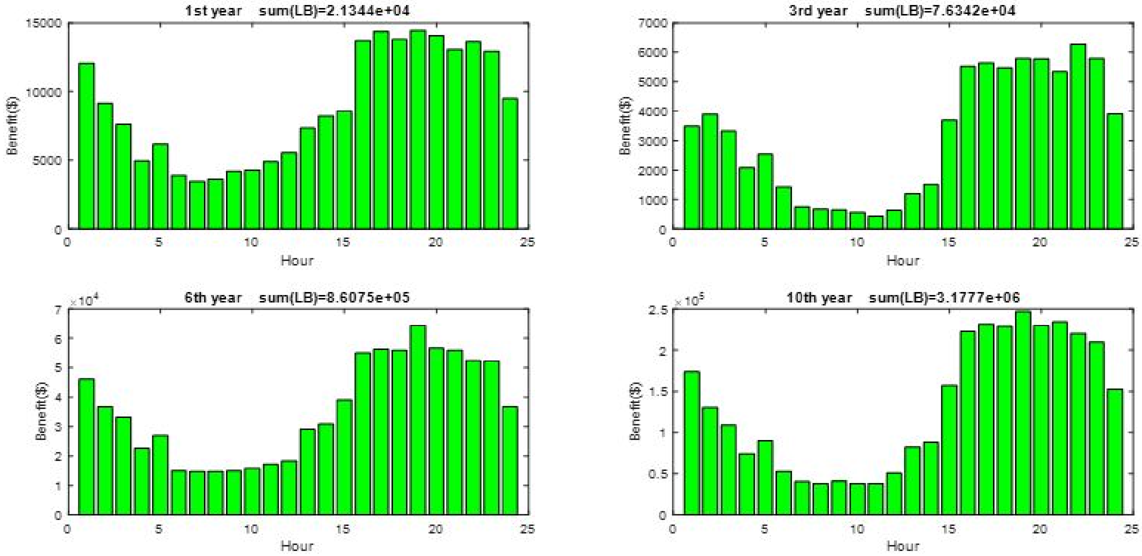

Figure 13: Benefits from the reduce active losses in a short time (with CS and WG)

In objective functions, the profit partly comes from the upstream network power, as presented in Figure 14. The profit was assessed in four periods; however, the system reached the highest profit during the 10th year. In this regard, CS and WGs are also present in the 10th year, resulting in significant profits.

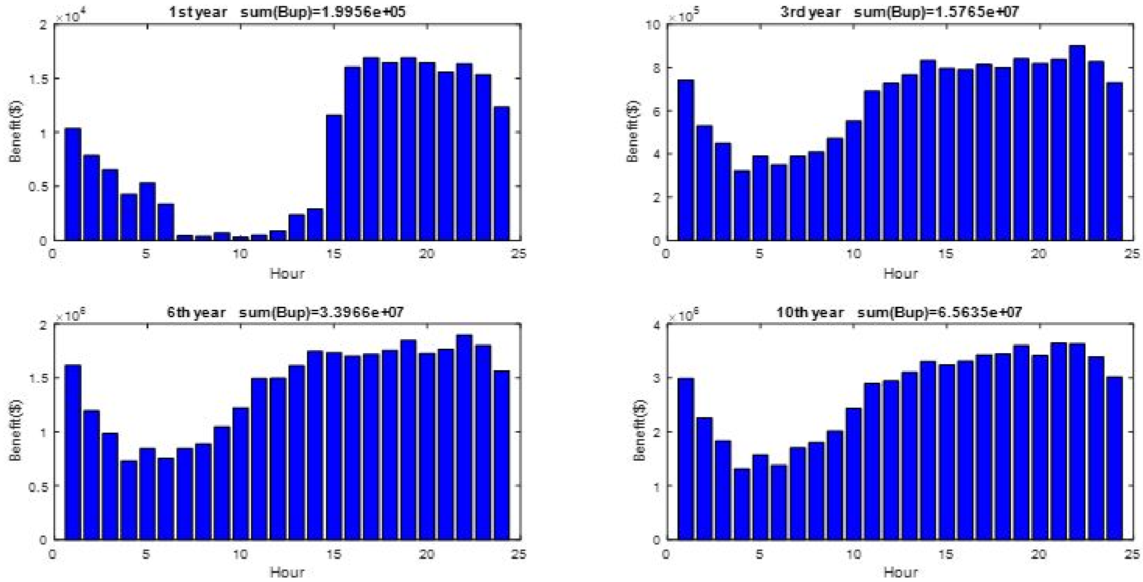

Figure 14: Benefits from upstream function in a short time (with CS and WG)

Figure 15 shows the voltage profiles for nine buses. Voltage profile exhibits better results and less oscillation in the tenth year, compared to the other years. Figure 16 (a) shows the voltage profile of busses with no CS and WG. Better results are obtained for this profile in the tenth year (Figure 15). The effect of CS and DG on the voltage profile is obvious as the profit from the reliability function decreases in the absence of CS and WG during the 10th year (Figure 16 (b)).

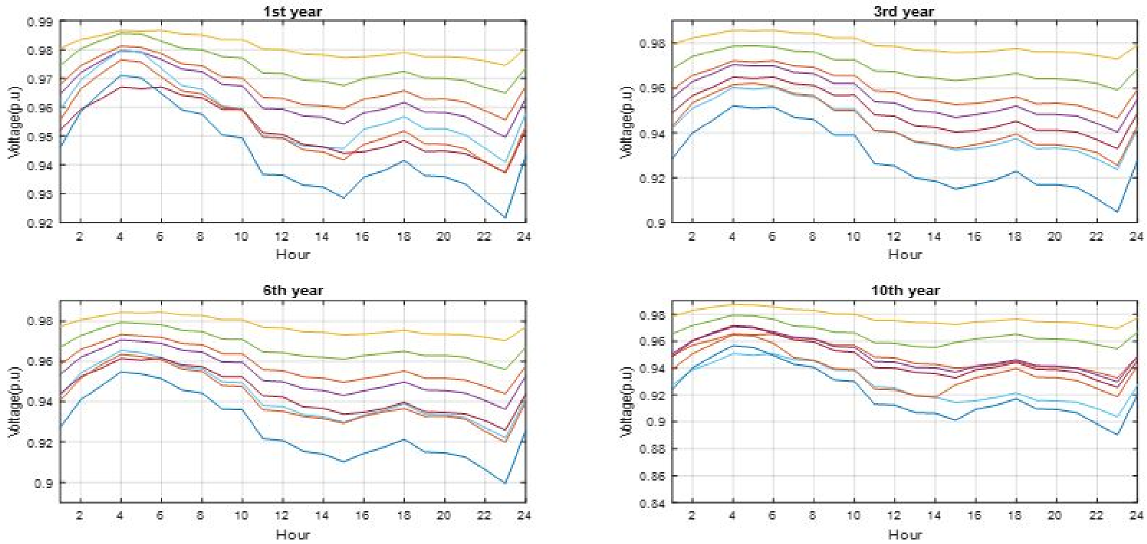

Figure 15: Busses' voltage profile in a short time (with CS and WG)

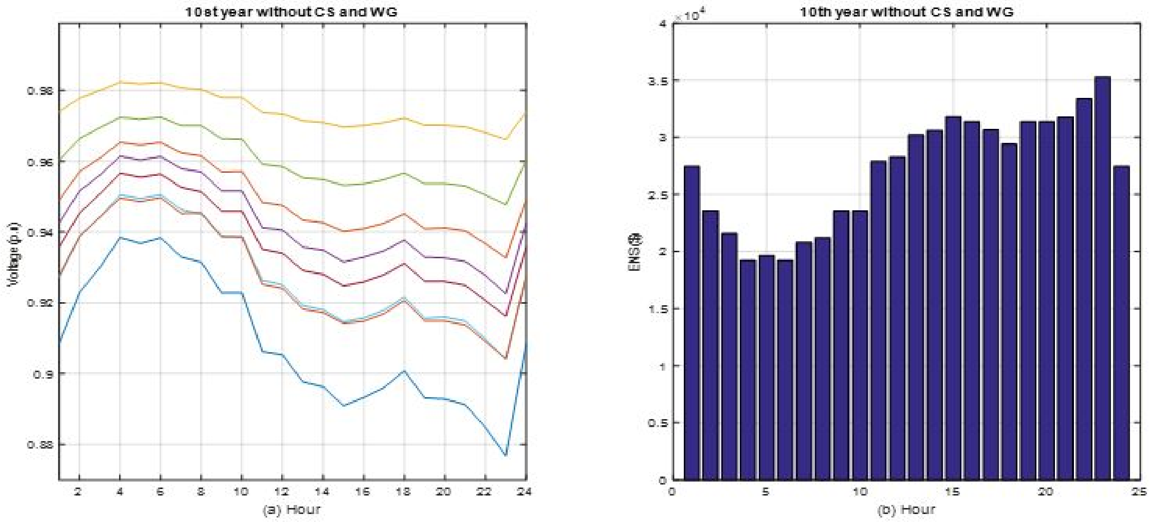

Figure 16: (a) Busses' voltage profile in a short time (without CS and WG), (b) Benefits from reliability function (without CS and WG)

5. Conclusion

Regarding load uncertainty and electricity price uncertainty, a new model was proposed in this study. On the other hand, with regard to the variation of wind velocity, the joint contribution of obtained output power of wind units and the simultaneous programming of wind units and charging stations is economically justifiable, from which the distribution system earn the greatest benefits. In addition, charging station power was obtained according to the probabilistic behavior of the EV owners. In this paper, the BSA algorithm was applied to optimize the NSBSA implementation.This algorithm has not been modeled in energy systems.

References

[1] Annual Energy Outlook 2020. British Energy Information Administration; Independent statistics and analysis. London, England 2020. https://www.eia.gov/outlooks/aeo/

[2] J.C. Mukherjee, A. Gupta, Distributed charge scheduling of plug-in electric vehicles using inter-aggregator collaboration, IEEE Transactions on Smart Grid 8.1 (2017): 331-341.

[3] E. Chlebišová, J. Kyzeková, H. Svobodová, Marketing study of the electric vehicles diffusion, Proceeding of the 11th Scientific Conference Electric Power Engineering, EPE. 10 (2010): 807-811.

[4] K.M. Tan, V.K. Ramachandaramurthy, J.Y. Yong, Integration of electric vehicles in smart grid: A review on vehicle to grid technologies and optimization techniques, Renewable and Sustainable Energy Reviews 53 (2016): 720-732.

[5] S. Tabatabaee, S. Mortazavi, T. Niknam, Stochastic scheduling of local distribution systems considering high penetration of plug-in electric vehicles and renewable energy sources, Energy 2017; 121: 480-490. http://dx.doi.org/10.1016/j.energy.2016.12.115

[6] M.S. Shemami, M.S. Alam, M.J.Asghar, Reliable Residential Backup Power Control System Through Home to Plug-In Electric Vehicle (H2V), Technology and Economics of Smart Grids and Sustainable Energy 3.1 (2018): 8.

[7] A.G. Boulanger, A.C. Chu, S. Maxx, D.L. Waltz, Vehicle electrification: Status and issues, Proceedings of the IEEE 99.6 (2011): 1116-1138.

[8] O. Veneri, L. Ferraro, C. Capasso, D. Iannuzzi, Charging Infrastructures for EV: Overview of Technologies and Issues; IEEE 2012 ESARS, Electrical Systems for Aircraft, Railway and Ship Propulsion Conference; Bologna, Italy; 2012. http://dx.doi.org/ 10.1109/ESARS.2012.6387434

[9] M. Yilmaz, P.T. Krein, Review of battery charger topologies, charging power levels, and infrastructure for plug-in electric and hybrid vehicles, IEEE transactions on Power Electronics 28.5 (2012): 2151-2169.

[10] M. Brenna, M.C. Falvo, F. Foiadelli, L. Martirano, F. Massaro, D.A.V.I.D.E. Poli, A. Vaccaro, Challenges in energy systems for the smart-cities of the future, 2012 IEEE International Energy Conference and Exhibition (ENERGYCON). IEEE, 2012. doi.org/10.1109/EnergyCon.2012.6348251

[11] M.C. Falvo, L. Martirano, D. Sbordone, E. Bocci, Technologies for smart grids: A brief review, 2013 12th International Conference on Environment and Electrical Engineering. IEEE, 2013. http://dx.doi.org/ 10.1109/EEEIC.2013.6549544

[12] M.C. Falvo, L. Martirano, D. Sbordone, Sustainable energy microsystems for a smart grid, Neural Nets and Surroundings. Springer, Berlin, Heidelberg, (2013): 259-269. http://dx.doi.org/10.1007/978-3-642-35467-0_ 26

[13] L.P. Fernandez, T.G. San Roman, R. Cossent, C.M. Domingo, P. Frias, Assessment of the impact of plug-in electric vehicles on distribution networks, IEEE transactions on power systems 26.1 (2010): 206-213.

[14] M. Etezadi-Amoli, K. Choma, J. Stefani, Rapid-charge electric-vehicle stations, IEEE transactions on power delivery 25.3 (2010): 1883-1887.

[15] H. Hõimoja, A. Rufer, G. Dziechciaruk, A. Vezzini, An ultrafast EV charging station demonstrator, International Symposium on Power Electronics Power Electronics, Electrical Drives, Automation and Motion. IEEE, (2012): 1390-1395.

[16] D. Aggeler, F. Canales, H. Zelaya-De La Parra, A. Coccia, N. Butcher, O. Apeldoorn, Ultra-fast DC-charge infrastructures for EV-mobility and future smart grids, 2010 IEEE PES Innovative Smart Grid Technologies Conference Europe (ISGT Europe). IEEE, 2010. http://dx.doi.org/10.1109/ISGTEUROPE.2010.5638899

[17] S. Bai, D. Yu, S. Lukic, Optimum design of an EV/PHEV charging station with DC bus and storage system." 2010 IEEE Energy Conversion Congress and Exposition. IEEE, (2010): 1178-1184.

[18] H. Fredriksson, M. Dahl, J. Holmgren. Optimal placement of charging stations for electric vehicles in large-scale transportation networks, Procedia Computer Science 160 (2019): 77-84. http://dx.doi.org/10.1016/j.procs.2019.09.446

[19] J. He, H. Yang, T.Q. Tang, H.J. Huang An optimal charging station location model with the consideration of electric vehicle's driving range, Transportation Research Part C: Emerging Technologies 86 (2018): 641-654.

[20] W. Kempton, S. Letendre, Electric vehicles as a new power source for electric utilities; Transportation Research Part D: Transport and Environment, 2 (1997): 157-175. http://dx.doi.org/org/10.1016/S1361-9209(97)00001-1

[21] T. Katrasnik, Energy conversion phenomena in plug-in hybrid-electric vehicles. Energy Conversion and Management 52 (2011): 2637-2650. http://dx.doi.org/ 10.1016/j.enconman.2011.01.025

[22] X. Li, J. Cao, D. Du, Comparison of Levenberg-Marquardt Method and Path Following Interior Point Method for the Solution of Optimal Power Flow Problem, International Journal of Emerging Electric Power Systems 13.3 (2012). http://dx.doi.org/10.1515/1553-779X.2892

[23] L. Dong, W. Cheng, H. Bao, Y. Yang, Probabilistic Load Flow Analysis for Power System Containing Wind Farms.In: Asia-Pacific Power and Energy Engineering Conference; Chengdu, China; (2010): 1–4. http://dx.doi.org/10.1109/APPEEC.2010.5448900

[24] Y. Huang, Q. Xu, Y. Yang, X. Jiang, Numerical method for probabilistic load flow computation with multiple

correlated random variables." IET Renewable Power Generation 12.11 (2018): 1295-1303.

[25] A. Soroudi, R. Caire, N. Hadjsaid, M. Ehsan, Probabilistic dynamic multiobjective model for renewable and non-renewable distributed generation planning. IET Generation, Transmission & Distribution, 5 (2011): 1173-1182. http://dx.doi.org/10.1049/iet-gtd.2011.0173

[26] M. Moradijoz, M. ParsaMoghaddam, M. Haghifam, E. Alishahi, A multiobjective optimization problem for allocating parking lots in a distribution network. International Journal of Electrical Power & Energy Systems, 46 (2013): 115-122. http://dx.doi.org/10.1016/j.ijepes.2012.10.041

[27] W. Su, M. Chow, Performance evaluation of an EDA-based largescale plug-in hybrid electric vehicle charging algorithm. IEEE Transactions on Smart Grid, 3 (2011): 308-315. http://dx.doi.org/10.1109/TSG.2011.2151888

[28] Y. Khalid, J. Majeed, Probabilistic Modeling of Plug-In Electric Vehicle Charging Impacts on Power Systems. Energy and Environment 2010; University of Chalmers, 2010.

[29] M. AlRashidi, M. AlHajri, Optimal planning of multiple distributed generation sources in distribution networks; Energy Conversion and Management, 52 (2011): 3301-3308. http://dx.doi.org/10.1016/j.enconman.2011.06.001

[30] B. Yousefi-khangah, S. Ghassemzadeh, S.H. Hosseini, B. Mohammadi-Ivatloo, Short-term scheduling problem in smart grid considering reliability improvement in bad weather conditions, IET Generation, Transmission & Distribution, 11 (2017): 2521–2533. http://dx.doi.org/10.1049/iet-gtd.2016.1261.

[31] M. Mazidi, A. Zakariazadeh, S.H. Jadid, S. Pierluigi, Integrated scheduling of renewable generation and demand response programs in a microgrid. Energy Conversion and Management, 86 (2014): 1118-1127. http://dx.doi.org/10.1016/j.enconman.2014.06.078

[32] S. Shojaabadi, S. Abapour, M. Abapour, A. Nahavandi, Simultaneous planning of plug-in hybrid electric vehicle charging stations and wind power generation in distribution networks considering uncertainties; Renewable Energy, 99 (2016): 237-252. http://dx.doi.org/10.1016/j.renene.2016.06.032.

[33] N. Khalesi, N. Rezaei, M.R. Haghifam, DG allocation with application of dynamic programming for loss reduction and reliability improvement. International Journal of Electrical Power & Energy Systems, 33 (2011): 288-295. http://dx.doi.org/10.1016/j.ijepes.2010.08.024

[34] K. Khalkhali, S. Abapour, M. Moghaddas, M. Abapour, Application of data envelopment analysis theorem in plug-in hybrid electric vehicle charging station planning. IET Generation, Transmission & Distribution, 9 (2014): 666–676. http://dx.doi.org/ 10.1049/iet-gtd.2014.0554

[35] K. Deb, A. Pratap, S. Agarwal, A fast and elitist multiobjective genetic algorithm: Nsga-II. IEEE Transactions on Evolutionary Computation, 6 (2002): 182–197. http://dx.doi.org/ https://doi.org/10.1109/4235.996017

[36] A. Soroudi, M. Ehsan, R. Caire, N. Hadjsaid, Hybrid immune-genetic algorithm method for benefit maximisation of distribution network operators and distributed generation owners in a deregulated environment. IET Generation, Transmission & Distribution, 5 (2011): 961-972. http://dx.doi.org/10.1049/iet-gtd.2010.0721

[37] L.P. Fernandez, T.G. San Roman, R. Cossent, C.M. Domingo, P. Frías, Assessment of the Impact of Plug-in Electric Vehicles on Distribution Networks. IEEE Transactions on Power Systems, 26 (2011): 206-213. http://dx.doi.org/ 10.1109/TPWRS.2010.2049133

[38] V.H. Quintana, H.K. Temraz, K.W. Hipel, Two-stage power system distribution planning algorithm, IEE Proceedings C (Generation, Transmission and Distribution) 140 (1993): 17–29. http://dx.doi.org/10.1049/ip-c.1993.0004

[39] D. Singh, R.K. Misra, D. Singh, Effect of load models in distributed generation planning, IEEE Transactions on Power Systems, 22 (2007): 2204-2212. http://dx.doi.org/ 10.1109/TPWRS.2007.907582

[40] P. Civicioglu, Backtracking Search Optimization Algorithm for numerical optimization problems. Applied Mathematics and Computation, 219 (2013): 8121–8144. http://dx.doi.org/10.1016/j.amc.2013.02.017

[41] Y. Puranik, N.V. Sahinidis, Domain reduction techniques for global NLP and MINLP optimization. Constraints springer Verlag, 22 (2017): 338-376. http://dx.doi.org/ 10.1007/s10601-016-9267-5.

[42] J. Branke, K. Deb, K. Miettinen, R. Slowinski, Multiobjective Optimization: Interactive and Evolutionary Approaches. Theorical computer science and general issues, New York, USA: Springer press, 2008.

[43] Sh. Ross, R. Weber, Multi-Objective Optimization using Evolutionary Algorithms. West Sussex, England: Wiley press, 2001.